Atmos. Chem. Phys., 9, 4973–4985, 2009
www.atmos-chem-phys.net/9/4973/2009/

Atmospheric Chemistry and Physics

Sources and transport of $\Delta^{14}C$ in CO_2 within the Mexico City Basin and vicinity

S. A. Vay[1], S. C. Tyler[2], Y. Choi[3], D. R. Blake[2], N. J. Blake[2], G. W. Sachse[3], G. S. Diskin[1], and H. B. Singh[4]

[1]NASA Langley Research Center, Hampton, Virginia, USA
[2]University of California, Irvine, California, USA
[3]National Institutes of Aerospace, Hampton, Virginia, USA
[4]NASA Ames Research Center, Moffett Field, California, USA

Received: 2 March 2009 – Published in Atmos. Chem. Phys. Discuss.: 17 March 2009
Revised: 16 July 2009 – Accepted: 20 July 2009 – Published: 27 July 2009

Abstract. Radiocarbon samples taken over Mexico City and the surrounding region during the MILAGRO field campaign in March 2006 exhibited an unexpected distribution: (1) relatively few samples (23%) were below the North American free tropospheric background value (57±2‰) despite the fossil fuel emissions from one of the world's most highly polluted environments; and (2) frequent enrichment well above the background value was observed. Correlate source tracer species and air transport characteristics were examined to elucidate influences on the radiocarbon distribution. Our analysis suggests that a combination of radiocarbon sources biased the "regional radiocarbon background" above the North American value thereby decreasing the apparent fossil fuel signature. Likely sources include the release of ^{14}C-enhanced carbon from bomb ^{14}C sequestered in plant carbon pools via the ubiquitous biomass burning in the region as well as the direct release of radiocarbon as CO_2 from other "hot" sources. Plausible perturbations from local point "hot" sources include the burning of hazardous waste in cement kilns; medical waste incineration; and emissions from the Laguna Verde Nuclear Power Plant. These observations provide insight into the use of $\Delta^{14}CO_2$ to constrain fossil fuel emissions in the megacity environment, indicating that underestimation of the fossil fuel contribution to the CO_2 flux is likely wherever biomass burning coexists with urban emissions and is unaccounted for as a source of the elevated CO_2 observed above local background. Our findings increase the complexity required to quantify fossil fuel-derived CO_2 in source-rich environments characteristic of megacities, and have implications for the use of $\Delta^{14}CO_2$ observations in evaluating bottom-up emission inventories and their reliability as a tool for validating national emission claims of CO_2 within the framework of the Kyoto Protocol.

Correspondence to: S. A. Vay
(stephanie.a.vay@nasa.gov)

1 Introduction

With over 10 million inhabitants, megacities are a major source of air pollution given their high traffic densities, energy consumption rates, industrial processes, and elevated levels of biomass combustion from land clearing, trash burning and both domestic and industrial use of wood fuels (Gaffney et al., 2008). Emissions from megacities located within developing countries can differ from US and European cities as less stringent regulations allow higher levels of more complex gases and aerosols to be emitted (Raga et al., 2001). As their number increases worldwide, there is a growing recognition that airborne emissions from these large urban and industrial centers change the chemical content of the downwind troposphere, influencing both air quality and climate change on multiple scales (Molina et al., 2008).

The Mexico City metropolitan area (MCMA) is the second largest megacity worldwide, the most populous city in North America, and was the initial case study for MILAGRO (Megacity Initiative: Local And Global Research Observations); an international collaborative project to examine the behavior and export of atmospheric pollutants generated in megacities. The interaction of physical and cultural factors in

the Valley of Mexico and surrounding region creates a spectrum of air pollutants extremely diverse in chemical characteristics (deBauer and Krupa, 1990; Collins and Scott, 1993). The NASA DC-8 was one of seven instrumented research aircraft participating in MILAGRO, providing in situ and remote observations of trace gases and aerosols from a regional-scale perspective. Instrumentation for measurement of carbon dioxide and the collection of whole air samples for radiocarbon analyses was integrated on the DC-8 to investigate the various local and regional sources contributing to the measured total atmospheric CO_2 signal.

Anthropogenic perturbations, mainly attributable to land-use changes, fossil fuel burning, and atmospheric nuclear detonations, have markedly affected the natural balance of the ^{14}C in CO_2 cycle (Suess, 1955; Tans et al., 1979; Stuiver and Quay, 1981; Rozanski et al., 1995; and Caldeira et al., 1998). The isotopic analysis of CO_2 in the lower atmosphere has resulted in a better understanding of the ^{14}C exchange with the biosphere and the role of anthropogenic activity (Zondervan and Meijer, 1996; Dutta et al., 2002). More than 40 years of direct tropospheric $^{14}CO_2$ observations from maritime and continental stations in both hemispheres are now available since the nuclear test ban treaty in 1962 (Mook, 1980; Rozanski et al., 1995; Levin and Hesshaimer, 2000; Kitagawa et al., 2004). Seasonal and regional variability in atmospheric $\Delta^{14}C$ is clearly visible in many contemporary observations and has the potential to provide additional information about the source, age, and magnitude of regional fluxes (Randerson et al. 2002).

The direct effect of fossil fuel emissions is arguably the most significant influence of urbanization on the carbon cycle (Pataki et al., 2006). $\Delta^{14}C$ is a particularly sensitive tracer of fossil fuel emissions (Hsueh et al., 2007) because fossil fuel-derived CO_2 is the only source of atmospheric CO_2 that is devoid of ^{14}C (Suess, 1955; Levin et al., 1980; Turnbull et al., 2009). When combined with atmospheric CO_2concentration measurements, observations of $\Delta^{14}C$ can potentially be used to constrain fossil fuel emissions at local and regional scales. Quantifying fossil fuel CO_2 emissions by isotopic analysis requires knowledge of the clean air isotopic composition (Levin et al., 1980). A measured $^{14}C/^{12}C$ ratio below the background value has been used to directly yield the fraction of fossil fuel CO_2 (Levin et al., 1980; Zondervan and Meijer, 1996).

The purpose of this paper is to present insight into the processes regulating the distribution of atmospheric $\Delta^{14}C$ in the MCMA environment in March 2006, and to discuss the implications of those measurements as they pertain to alterations to the carbon cycle and the quantification of anthropogenic carbon sources.

2 Methods

2.1 Field deployments

In 2006, NASA's Tropospheric Chemistry Program (TCP) sponsored the INTEX-B (Intercontinental Chemical Transport Experiment-B) mission which consisted of two separate field deployments. The initial phase investigated the extent and persistence of outflow of pollution from Mexico during MILAGRO (1–30 March 2006) with flights based out of Houston, Texas (4–19 March 2006). The DC-8 then transited to Moffett Field, California, and after a three-week break, began making measurements over the North Pacific to quantify the impact of the long-range transport of accelerating Asian emissions on the changing chemical composition of the troposphere. The DC-8 conducted three local flights out of Honolulu, Hawaii followed by four local sorties out of Anchorage, Alaska. This study focuses on data obtained from the Houston-based flights and invokes the transit flight data over the North Pacific. Data from the local flights out of Hawaii and Alaska are the topic of a forthcoming manuscript.

2.2 Airborne measurements

A modified LI-COR model 6252 non-dispersive infrared gas analyzer was used to determine CO_2 mixing ratios. This dual-cell instrument achieves high precision by measuring the differential absorption between sample air and a calibrated reference gas that is traceable to the World Meteorological Organization primary CO_2 standards maintained by NOAA ESRL. The LI-COR-based CO_2 sampling system was operated at constant pressure (250 torr) and had a precision of ± 0.1 ppm (1σ) and accuracy of ± 0.25 ppm. Experimental procedures are described in detail by Anderson et al. (1996) and Vay et al. (1999, 2003). The MILAGRO/INTEX-B in situ CO_2 data are archived at 1 s resolution and are publically available via http://www-air.larc.nasa.gov.

The ^{14}C content of CO_2 was determined from air remaining in a select subset of whole air canister samples collected onboard the DC-8 for measurements of hydrocarbons and halocarbons (Blake and Rowland, 1995). Our radiocarbon sample collection strategy targeted pollution events in an attempt to quantify fossil fuel CO_2. Pollution plumes were identified by enhancements in various chemical tracers measured in real-time onboard the DC-8. Post-mission, measurements of the radiocarbon content on CO_2 were made at the W. M. Keck Carbon Isotope Accelerator Mass Spectrometer Facility at the University of CA-Irvine and are described below.

Complementary data used here from numerous instruments has a long history of inclusion in the NASA DC-8 TCP payload, and the techniques were essentially identical to those previously described by Sachse et al. (1988); Blake et al. (1996); and Singh et al. (2003). Our multi-tracer analysis utilized data for CO, CH_4, C_2H_6, C_2Cl_4, CH_3CN, HCN,

isoprene and isopentane. An overview of the mission is given by Molina et al. (2008) and Singh et al. (2009).

2.3 Analytical procedures

Aliquots of air for radiocarbon CO_2 analyses were taken from sample canisters after all other hydrocarbon measurements were completed. In the selected canisters, 70 to 140 kPa above atmospheric pressure was left post hydrocarbon analyses easily allowing for aliquots to be withdrawn for radiocarbon analyses with an optimum sample size for high precision $\Delta^{14}C$ measurements, i.e., ca. 1000 uL CO_2 gas at STP which provides ca. 0.5 mg C target for AMS analysis.

Preparation of the samples for isotopic analysis was done on a combustion vacuum line that separates CH_4, CO, and CO_2 trace gases from whole air (and from each other) while further converting CH_4 to CO_2 and H_2O and converting CO to CO_2 as the air stream moves toward the pump. Most of the details regarding the vacuum line design and procedure as well as improvements made over time have been reported previously (Tyler et al., 1999 and references therein). In this study, only the CO_2 fraction from the total air sample was recovered. In brief, for a given sample, a series of cryo traps condensed trace gases such as CO_2 and H_2O vapor at liquid N_2 temperature ($-196°C$), leaving less-readily condensable gases such as CO and CH_4 in the air stream. The CO_2 was then separated from H_2O using a dry ice/ethanol slush bath ($-80°C$) and saved for isotopic analysis.

Measurements of ^{14}C content in samples of CO_2 from selected air samples were made following previously described methods (Southon et al., 2003). Briefly, CO_2 gas is graphitized to pure carbon in the presence of H_2 and hot zinc metal. From there, graphite targets are formed and then mounted into a sample target wheel where they are subsequently measured in the accelerator mass spectrometer. Overall $\Delta^{14}C$ measurement precision is ±2‰ or ±0.2 percent Modern Carbon, where $\Delta^{14}C$ and pMC are defined by Stuiver and Polach (1977).

Repeated tests of radiocarbon dead CO_2 from either old coal or calcite were made along with the air sample analyses. These ^{14}C-free calibration samples were provided by the Keck AMS facility and have a sample size of ca. 1000 uL CO_2 gas at STP, which closely matched the size of the unknown CO_2 in the air samples measured. Some of these calibration blanks were introduced directly into the vacuum line used to recover CO_2 in the samples, while others were introduced as pseudo-air samples by first injecting them into randomly selected canisters from D. Blake's research group and pressurizing to ca. 105 kPa with Zero Air to ascertain whether his sample vessels could have a high background of ^{14}C from previous usage on other projects. Our vacuum line blank was $\Delta^{14}C$=-995±2‰ (0.5±0.2 pMC), a value consistent with other low blank determinations made in years past in our lab. Note that this value includes the quoted Keck AMS measurement precision of ±2‰ and is the combined blank and uncertainty from sampling, processing, graphitizing, and measuring ^{14}C content. It should be pointed out that the exact age of either the calcite or graphite derived calibration gases is not known. In the past we have analyzed natural gas from petroleum deposits and determined values as low as $\Delta^{14}C$=−999 to −1001‰ (−0.1 to +0.1 pMC), indicating that total sample blank from vacuum line may be even lower than the value listed above.

2.4 Clean air isotopic composition

The INTEX-B transit flight data from Moffett Field, California to Honolulu, Hawaii (17 April 2006) and from Honolulu to Anchorage, Alaska (30 April 2006) are invoked to obtain a representative background radiocarbon value of 57±2‰ for this study. This value is in good agreement with a mean March 2006 $\Delta^{14}C$ value of 56.6‰ determined from observations at Niwot Ridge, Colorado (40° N, 105° W, 3526 m a.s.l.), a proxy for North American free tropospheric air (Turnbull et al., 2007).

Though this background value is determined from mid-latitude observations (32–43° N), 57±2‰ is our best assessment of the clean air isotopic composition based on available data. The monitoring network for ^{14}C within the tropical Northern Hemisphere is very sparse; the closest station to Mexico being Izana, Tenerife (8° N) located ∼300 km west of the African coast (March 2006 data are unavailable, I. Levin, personal communication, 2009). Earlier observations by Rozanski et al. (1995) and Levin and Hesshaimer (2000) revealed <4‰ difference between $^{14}CO_2$ levels within the Northern Hemisphere tropical troposphere compared to mid-latitudes. Hsueh et al. (2007) reported one $^{14}CO_2$ measurement from Mexico in a non-polluted setting near Tapalpa (19° N, 103° W) in July 2004 of 64.6‰; the corresponding July 2004 value reported for Niwot Ridge was 65.3‰ i.e. less than 1‰ difference between 19° N and 40° N values.

2.5 Mixing model

Raw data measurement results for the MILAGRO phase of INTEX-B appear in Table 1. For the 21 samples collected, the background ^{14}C content in CO_2 over Mexico City and from the surrounding region had a surprisingly high average value of ca. 72±26‰ (2σ)=$\Delta^{14}C$ (107.2±2.6 pMC). Several had ^{14}C values much higher than background for ^{14}C ($>1\sigma$ outside mean). This result was quite unexpected as these samples also had elevated CO_2 concentration above background level, an observation which is normally associated with fossil fuel sources in urban regions and would necessarily lead to depleted rather than elevated ^{14}C content. In comparison, our results for 22 whole air samples collected during the North Pacific phase of INTEX-B in April and May 2006 indicated that the background ^{14}C content in CO_2 was ca. 59±6‰ (2σ)=$\Delta^{14}C$ (105.9±0.6 percent Modern

Table 1. Samples collected over the Mexico City airshed.

Date Collected	$D^{14}C$ ‰	pMC %	CO_2 ppmv	CO ppbv	CH_4 ppbv	C_2Cl_4 pptv	i-pentane pptv	isoprene pptv	ACN pptv	HCN pptv	C_2H_6 pptv	ALT_R km	ALT_P km
3/9/2006	69	106.9	387.7	134	1852	4	68	32	147	438	1165	0.15	0.23
3/9/2006	66	106.6	388.7	138	1868	5	127	15	119	340	1360	0.16	0.23
3/9/2006	63	106.3	390.6	143	1890	4	212	<DL	119	340	1737	0.17	0.23
3/9/2006	59	105.9	392.2	150	1923	5	316	<DL	135	328	2996	0.15	0.22
3/9/2006	53	105.3	398.5	187	1925	7	311	<DL	182	582	5371	0.15	0.25
3/9/2006	69	106.9	395.9	184	1939	5	242	<DL	124	514	2931	0.15	0.25
3/11/2006	72	107.2	386.1	128	1807	3	7	<DL	121	334	786	0.31	0.32
3/11/2006	47	104.7	394.9	910	2470	308	7767	47	243	1346	2499	0.32	2.47
3/11/2006	66	106.6	390.3	158	1848	5	73	140	240	455	993	0.27	0.34
3/16/2006	95	109.5	386.8	230	1835	31	347	<DL	152	980	1415	1.60	2.64
3/16/2006	77	107.7	386.8	221	1834	25	293	<DL	152	980	1263	1.43	2.61
3/16/2006	79	107.9	386.5	210	1830	38	351	<DL	−999	−999	1308	1.45	2.62
3/16/2006	120	112.0	388.1	384	1837	40	1612	69	263	2749	1637	0.76	2.62
3/16/2006	20	102.0	405.6	1207	2134	509	8672	53	491	3381	5423	0.58	2.69
3/16/2006	49	104.9	395.1	681	1983	255	3625	27	491	3381	3329	0.55	2.62
3/16/2006	50	105.0	395.8	220	1876	7	233	308	159	1136	3213	0.63	0.92
3/16/2006	79	107.9	390.3	197	1869	6	175	223	292	999	2911	0.35	0.38
3/19/2006	66	106.6	384.0	151	1828	5	81	<DL	214	819	1137	0.75	0.79
3/19/2006	132	113.2	384.6	199	1835	9	233	4	293	1504	1146	1.49	2.57
3/19/2006	62	106.2	383.5	210	1825	6	567	9	131	275	972	0.43	2.57
3/19/2006	113	111.3	385.4	200	1816	8	617	43	216	1114	1361	0.56	1.05

Representative March surface background concentrations (and atmospheric lifetimes) for C_2Cl_4 ($\tau\sim$1 day), CH_3CN ($\tau>$few months), HCN ($\tau>$few months), and C_2H_6 ($\tau\sim$3 months) are 3 pptv, 100 pptv, 140 pptv, and 750 pptv, respectively. Background<detection limit (DL) for isoprene ($\tau<$1 h) and isopentane ($\tau\sim$1 h). Radar (ALT_R) and pressure (ALT_P) altitude.

Carbon). This is in excellent agreement with recent Northern Hemispheric studies of background CO_2 in air (Levin and Kromer, 2004; Xu et al., 2004, 2006) that indicate a level of between 105 to 106 pMC over the whole year by direct monitoring at specific sites.

Many of the air samples measured over Mexico indicate that we potentially have at least two CO_2 sources contributing to the elevated CO_2 mixing ratios observed in those cases. For example, one can see the need for two sources most readily by a simple calculation made for the three samples with lowest measured $\Delta^{14}C$ values in Table 1. Assuming background air is affected by only one source, fossil fuel, one would expect the excess CO_2 above background to have only a radiocarbon dead $\Delta^{14}C$ signature. Equations (1) and (2) can be used to calculate the expected value of $\Delta^{14}C$ in the sample air when fossil fuel CO_2 is added to the background.

$$S_{BKGR} + S_{FF} = S_{TOT} \quad (1)$$

$$(1 - S_{FF}) \times \Delta^{14}C_{BKGR} + S_{BKGR} \times \Delta^{14}C_{FF} = S_{TOT} \times \Delta^{14}C_{SAM} \quad (2)$$

Using background values of 382.8 ppmv and 57‰ for mixing ratio and $\Delta^{14}C$ of CO_2 to conform to Northern Hemispheric averages measured in March 2006 by others and a $\Delta^{14}C_{FF}$ value of −1000‰ (radiocarbon dead), one calculates that the three measured values of $\Delta^{14}C$ at 20, 47, and 49‰ would have to have been much lower. Hence, a mixture of both radiocarbon dead and radiocarbon enhanced sources would reasonably lead mathematically to the 3 values listed above.

Similarly, our measured values of $\Delta^{14}CO_2$ much above the background value must necessarily include source contributions from a radiocarbon enhanced source such as biomass burning (which was observed extensively in the region and could easily contain a slightly higher ^{14}C than modern background air depending on the biomass age) to balance any radiocarbon dead contribution from fossil fuels. Yet another possibility is that the air contains a very small amount of an appreciably "hotter" ^{14}C source such as medical waste released as $^{14}CO_2$. In this case the excess CO_2 mixing ratio from the hot source could be very small with most of the excess attributable to fossil fuel CO_2 source and yet the $\Delta^{14}C$ value would remain elevated above background from the very "hot" ^{14}C source.

To analyze our results further we constructed a two-component CO_2 source mixture equation with sources both ^{14}C-depleted and ^{14}C-enhanced contributing to a CO_2

background of well-mixed air which makes up the majority of the sample. Calculations partitioning burning biomass (BIO) and fossil fuel (FF) sources of CO_2 can be made using Eqs. (3) and (4) below.

$$S_{BKGD} + S_{SOURCE} = S_{TOT} \quad (3)$$
$$(\text{where } S_{SOURCE} = S_{BIO} + S_{FF})$$

$$S_{BKGD} \times \Delta^{14}C_{BKGR} + (S_{SOURCE} - S_{BIO}) \quad (4)$$
$$\times -1000‰ + S_{BIO} \times 499‰ = S_{TOT} \times \Delta^{14}C_{TOT}$$

Assigning exact values to the radiocarbon-enhanced source is problematic because we are uncertain what that source is. Assuming that CO_2 from biomass burning of recent wood is the main source of ^{14}C-enhanced CO_2 in the region is a reasonable one based on visual observation and supporting data of other HC measurements. In that case, endpoints for our two-point source mixing curve were chosen as $\Delta^{14}C$=−1000‰ for fossil fuel and $\Delta^{14}C$=499‰ for biomass, where 499‰ represents stored carbon of about 35 years ago with the imprint from bomb-test ^{14}C suddenly being released as CO_2.

For observed $\Delta^{14}C$ of CO_2 values <50‰ listed in Table 1, calculations made with Eqs. (3) and (4) yield very plausible partitioning between fossil fuel and biomass burning sources. In those three cases, the partitioning is close to 50:50 for the two at 47 and 49‰ while it is ca. 75:25 in favor of fossil fuel over biomass burning for the observed $\Delta^{14}C$ of CO_2 value at 20‰. The above calculations also yield a reasonable partitioning between biomass and fossil fuel source contributions for observed values of $\Delta^{14}C$ of CO_2 between 55 and 70‰. In those cases, most of the excess CO_2 is calculated as coming from the biomass burning source. (Note that other partitioning ratios are possible if the $\Delta^{14}C$ of CO_2 from biomass burning is taken to be a value other than 499‰.)

However, for samples >70‰ in $\Delta^{14}C$, we have some physically impossible splits between the two types of sources in most cases. The problem stems from the fact that many of the observed $\Delta^{14}C$ of CO_2 values are very high even without much of an increase in the mixing ratio of CO_2 (only a few ppm) above background. In order to attribute enough source CO_2 to a ^{14}C-enhanced source, the fossil fuel contribution becomes negative in the partitioning which is impossible. This weakens our argument that the source of air with $\Delta^{14}C$>+100‰ can all be explained merely by somewhat aged wood from biomass burning.

One possible solution is to push the biomass age further back in time toward even higher assigned ^{14}C values, but there is a limit to this. The endpoint $\Delta^{14}C$ value for the biomass burning source in Eq. (4) is not really known, unlike the situation for most two-point mixing curves. We are estimating to obtain a fit however, since the bomb curve is not monotonically increasing backward in time but instead peaks ca. 1962, is skewed and is not even symmetric, pushing the estimated wood age back further is unrealistic as it

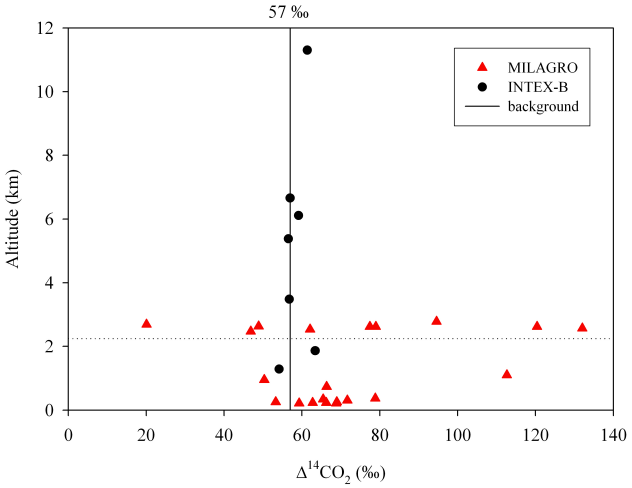

Fig. 1. Radiocarbon observations as a function of pressure altitude for the MILAGRO and INTEX-B North Pacific transit flights. Median radiocarbon measured over the eastern North Pacific was 57±2‰. Horizontal dotted line depicts the height of Mexico City (2240 m a.s.l.).

results in pre-bomb background $^{14}CO_2$ being stored in the biomass. Therefore we need to consider other possibilities as part of the mixture of contributing sources in the Mexico City region. These sources must be "hotter" than what we can reasonably expect from aged wood and are discussed in Sect. 3.3.

3 Large-scale distribution

The large-scale distribution of $\Delta^{14}C$ during MILAGRO and the INTEX-B Pacific transit flights is presented in Fig. 1. These data are shown as a function of pressure altitude since the MCMA lies in an elevated basin 2240 m a.s.l. Any anthropogenic emissions emitted from this megacity are therefore introduced into the atmosphere at altitudes considered to be in the free troposphere. An interesting feature of the MILAGRO ^{14}C data set is that 76% (N=16) of the radiocarbon values were above the assigned 57±2‰ background, with surprisingly few samples (N=5) indicating a fossil-fuel influence (<57‰). An anomalously high ^{14}C content (>112‰) was found in three of the collected samples and these results are examined in more detail in Sect. 3.3.

Canister sample collection locations and their associated radiocarbon values are illustrated in Fig. 2. This figure depicts the degree of spatial coverage within the region and provides a detailed look at the $\Delta^{14}C$ distribution. The flights on 9 and 16 March had different science objectives, sampling emissions over the Gulf of Mexico and Mexico City, respectively. We use these two flights to explore sources contributing to the total measured CO_2 signal in Sect. 3.1 and 3.2.

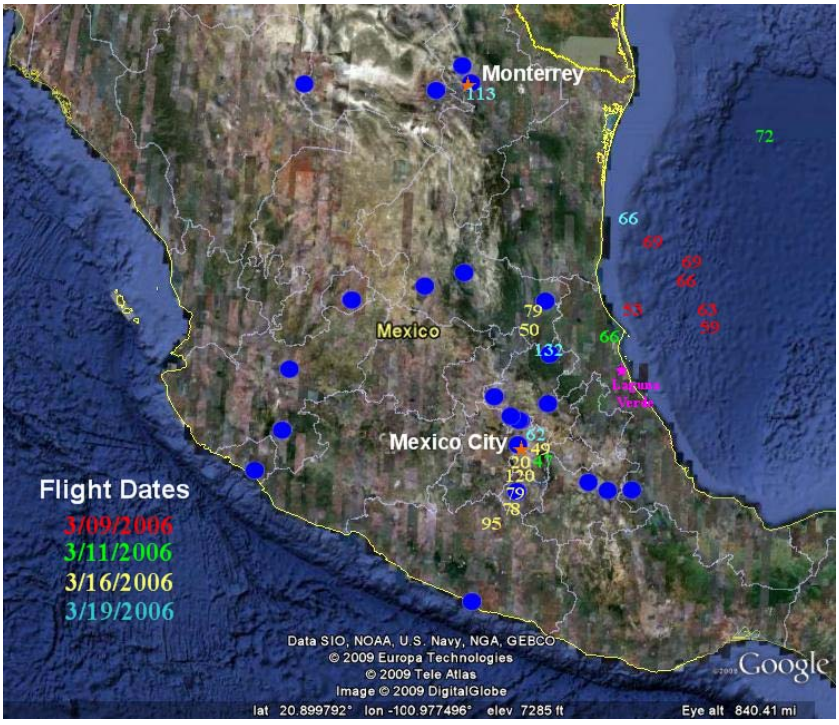

Fig. 2. Whole air sample collection locations and associated radiocarbon values color-coded by DC-8 flight date. Blue circular symbols represent locations of cement kilns.

3.1 Mexico City

An objective of the 16 March (Thursday) science flight was the sampling of fresh Mexico City (MC) pollution during weekday conditions. The flight track, altitude, and data for a portion of this flight are presented in Fig. 3. The DC-8 approached MC from the south, flew a south-north transect over the city along the same line of longitude, and then conducted a terrain-following path just north of the city. Collection sites for the isotope samples are indicated along the DC-8 flight track (blue diamonds). Inset above, in situ CO_2 and CO measurements are plotted with the $\Delta^{14}C$ observations. The radiocarbon values fell within the range of 20‰ to 120‰ with the lowest values observed directly over MC where the highest CO_2 and CO mixing ratios were measured. Using a $\Delta^{14}C$ depletion of 2.8‰ per ppm of fossil fuel CO_2 added to the current atmosphere (Turnbull et al., 2006), we estimate from our mixing model the minimum fossil fuel contribution to the total measured CO_2 signal to range between 4 to 15 ppm in the three samples lowest in $\Delta^{14}C$ value.

Collection of the isotope samples in clusters permitted partitioning of the flight segment into distinct regions labeled as A, B, C (Fig. 3). Regional correlations between CO_2 and CO are illustrated in Fig. 4. Following the method outlined in Yokelson et al. (1999) emission ratios (ERs) were obtained from the slope of the least-squares line, with the intercept forced to zero, in a plot of one set of excess mixing ratios versus another. Background values of 382.61 ppm and 112 ppb were used for CO_2 and CO, respectively based on the median determined from the four DC-8 flights. For comparison, median CO_2 and CO for Mauna Loa (19° N, 155° W, 3397 m a.s.l.) over the MILAGRO sampling window were 382.87 ppm and 105 ppb, respectively. Each cluster shows a distinct relationship, indicating a mixture of different sources that is also evident in the radiocarbon data.

Sampling over MC occurred during the January–June dry season. The level of fire activity in March 2006 was above normal and more typical of that seen in April. The Mexico City basin was influenced by emissions from forest fires in the pine-savannas that dominate the mountains surrounding the city (Yokelson et al., 2007). Both ground-based (E. Alvarado, personal communication, 2007) and airborne observers (DC-8 pilots, instrumentalists) reported reduced visibility from smoke generated by widespread wildfires and agricultural burning in South-Central Mexico that, at times, obscured the ground. The radiocarbon samples from south of Mexico City [Region A] were collected over the study area [19–20° N; 98–100° W] of Yokelson et al. (2007) who used a Twin Otter research aircraft to make various measurements of fire emissions during MILAGRO. We find that our CO:CO_2 molar emission ratio derived for Region A (0.024) compares well with Yokelson's (0.028) which was determined from measurements conducted the following day over a prescribed burn.

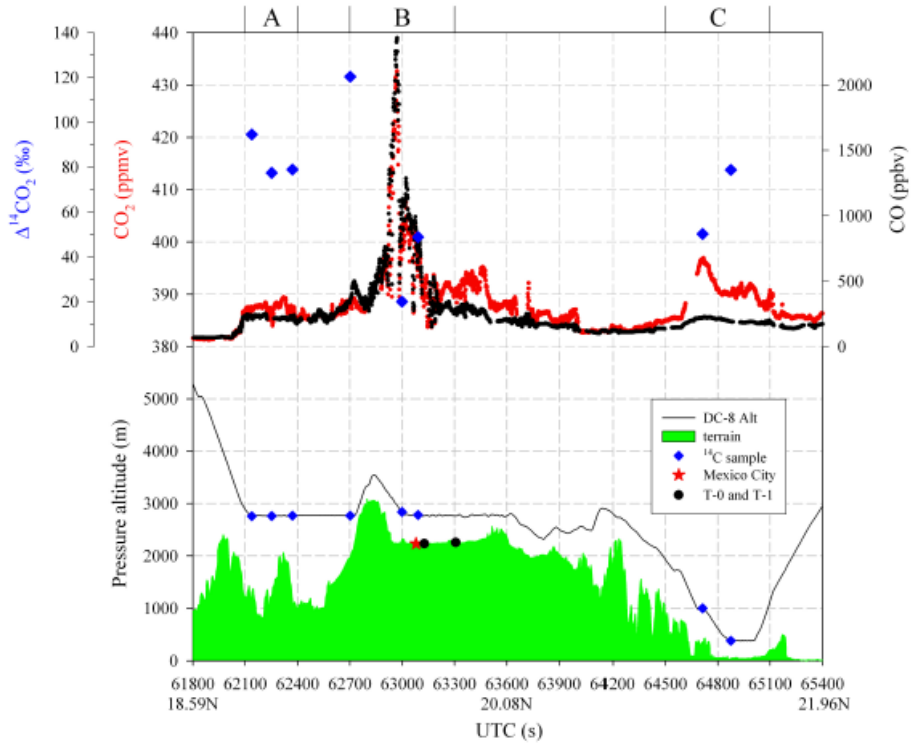

Fig. 3. Radiocarbon collection locations (blue diamonds) shown during a terrain-following flight track over Mexico City and vicinity on 16 March 2006 along with T0 and T1 ground-based MILAGRO super-sites (bottom panel). In situ CO_2 and CO data recorded during the flight with corresponding $\Delta^{14}CO_2$ values (top panel).

Several correlate source tracer species were examined to elucidate influences on the radiocarbon distribution: CH_3CN (also acetonitrile or ACN) and HCN (biomass burning); C_2Cl_4 (industrial emissions); isopentane (vehicular emissions); isoprene (biogenic emissions); and C_2H_6 (combustion from fossil fuels and biomass burning). Table 1 provides the mixing ratios, representative background values, and respective lifetimes for these tracers. For the short lived chemical tracers isopentane and isoprene ($\tau \leq 1$ h), any enhancements in these gases above their detection limits (DL) means that the air has been in very recent contact with a source region. In Fig. 5, the radiocarbon data are plotted along with several source tracers and reveal enhancements in ACN, isopentane, and C_2Cl_4 over all three regions; significant enrichment in C_2Cl_4 and isopentane over MC [Region B]; north of the city [Region C] isoprene mixing ratios >200 pptv were observed (not shown).

The pronounced influence of biomass burning on regional air quality during March 2006 is substantiated by several other MILAGRO investigations. Crounse et al. (2009) observed highly elevated concentrations of cyanides from measurements conducted onboard the NSF C-130 aircraft. Analysis of ^{14}C in aerosols collected at the MILAGRO ground-based super sites T-0 (19.488° N, 99.147° W, 2240 m a.s.l.) and T-1 (19.703° N, 98.982° W, 2273 m a.s.l.) (Fig. 2) revealed that significant contributions (45–78%) to the organic and elemental fractions of the carbonaceous aerosols arose from biomass burning sources in MC and the surrounding

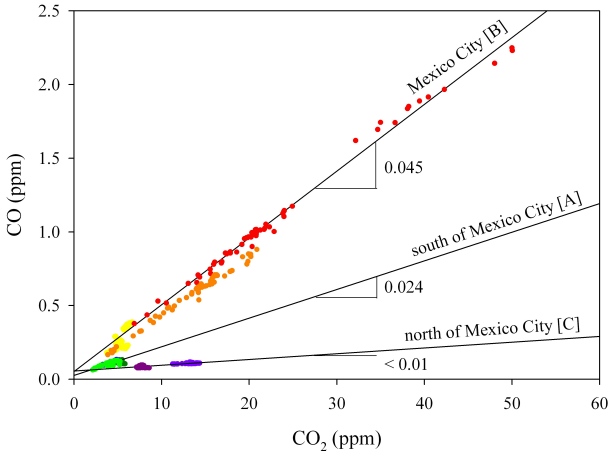

Fig. 4. Regional correlations between CO_2 and CO for radiocarbon sample collection intervals. Excess CO_2 and CO mixing ratios are plotted versus each other to obtain emission ratios by the method described in the text.

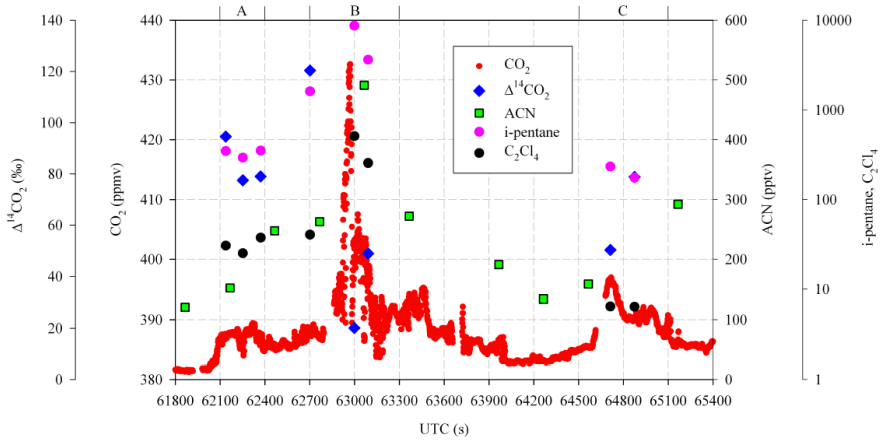

Fig. 5. Source tracer species concentrations for each radiocarbon sample collected on 16 March 2006. Note log scale for isopentane and C_2Cl_4.

region (Marley et al., 2009; Gaffney et al., 2008). Pyrogenic emissions greatly impacted the peripheral site T-1 as determined from ^{13}C in aerosol carbon observations that showed a number of plumes highly enriched in ^{13}C due to the pervasive burning of C4 grasses (Marley et al., 2009). Similarly, Stone et al. (2008) found that the aerosol generated by biomass burning on the perimeter of the city (T-1) was highly correlated with vegetative detritus and chemically different from the point-source wood-burning events that polluted the downtown area (T-0).

Fires emit significant amounts of CO_2 to the atmosphere with emission patterns that are highly variable in space and time (Wiedinmyer and Neff, 2007). Our data indicate that the ubiquitous biomass burning emissions during MILAGRO are a likely contributor to the mass excess in our $\Delta^{14}C$ observations via the re-suspension of radionuclides from contaminated biomass by fire. Using the variability in these observations to partition our two-point source mixing curve, we surmised that the age of carbon released to account for the excess mass would need to be from vegetation and soil organic matter that had fixed atmospheric CO_2 during the past several decades for a plausible fit. The fluxes from such events are important short-term influences on regional C patterns (Amiro et al., 2001) representing a challenge to the establishment of accurate C source and sink accounting based on atmospheric CO_2 observations (Wiedinmyer and Neff, 2007) alone.

3.2 Gulf of Mexico

On 9 March, the meteorological conditions were favorable for the sampling of outflow from Mexico City to the Gulf of Mexico. At takeoff the DC-8 climbed to 8.25 km, and then began descending while heading south over the Gulf in preparation for a boundary layer (BL) run. At this lowest level (∼200 m a.s.l.) the air masses had an unusual composition, containing high amounts of CH_4 (2.1 ppm) and CO_2 (400 ppm). CO_2, CO, and CH_4 observations, averaged to sampling time of the whole air samples, are presented in Fig. 6. The radiocarbon content of the four whole air samples collected during this southbound BL leg (triangular symbols in Fig. 6) show a decreasing trend as the DC-8 progressed further south (Fig. 2). As the CO_2, CH_4, and CO mixing ratios increase in these samples, the $\Delta^{14}C$ values become more depleted (Fig. 6). We were able to fit the data corresponding to these four $\Delta^{14}C$ samples with linear correlations that produced 0.285 ppmv/ppbv CO+349.63, R^2=0.98; and 0.068 ppmv/ppbv CH_4+262.15, R^2=0.98. These tight correlations likely reflect co-located sources. Examination of other source tracer species revealed $\Delta^{14}C$ correlated with ACN, HCN however, exhibiting the opposite relationship with isopentane and C_2H_6 (Table 1).

The largest natural gas and principal oil fields in Mexico are located around the Gulf of Mexico states of Veracruz, Tabasco, and Campeche. We use the Lagrangian particle dispersion model FLEXPART (Stohl et al., 1998) to explore the characteristics associated with meteorological transport processes in the region. Details of the model simulations are given by Stohl et al. (2002). Briefly, backward simulations are done from along the flight track and include full turbulence and convection parameterizations. Every simulation consists of 40 000 particles released in the volume of air sampled whenever the DC-8 covered a distance of 0.18° or changed its altitude by 8 hPa. As emissions originate at the surface, we focus on the residence times (ns/kg) in the FLEXPART regional footprint product, which shows the emission sensitivity averaged over the lowest 100 m adjacent to the ground. We also examined the Retroplume summary product to establish the fraction of particles in the BL as a function of time.

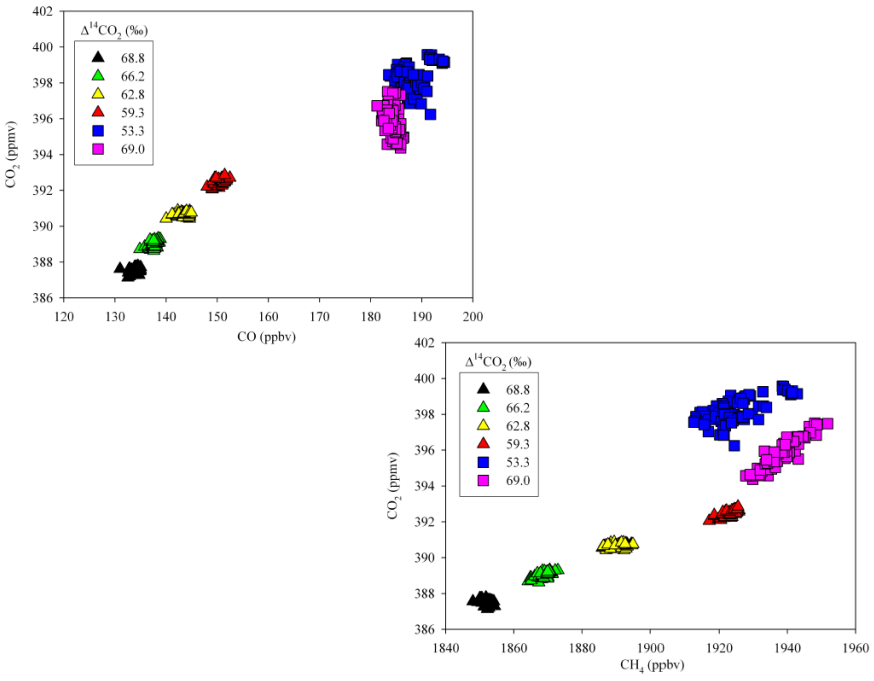

Fig. 6. Relationship of CO and CH_4 to CO_2 for the radiocarbon samples collected over the western Gulf of Mexico on 9 March 2006. The four samples collected during the southbound leg are represented by the triangular symbols; the squares symbolize the two samples collected closer to the coastline later that same day.

The air mass sampled in the BL during the southbound leg originated over northern Mexico, then flowed in a clockwise direction over the southern United States, the Gulf of Mexico, portions of Central America, and southern Mexico prior to interception over the Gulf (not shown). Inspection of Fig. 7 shows an initially narrow (Fig. 7a) influence footprint that broadens (Fig. 7b) with increasing proximity to the southern Mexico oil and gas center. A day prior to sampling, FLEXPART estimates an air mass fraction $\geq$60% traveling within the atmospheric boundary layer over the petroleum industry center as well as over fires in Guatemala and the Mexican states of Chiapas and Oaxaca. The corresponding decreasing trend of ACN, HCN, isoprene and $\Delta^{14}C$ while approaching the Mexican coastline with a commensurate increase in CO_2, CO, CH_4, C_2H_6, and isopentane suggests a biomass burning influence initially dominating the radiocarbon signal that became increasingly obscured by the influence of anthropogenic emissions associated with the petroleum industry. These results are supported by the FLEXPART emission sensitivity products (Fig. 7).

There are some notable differences in the composition of the two remaining BL (~200 m a.s.l.) samples (square symbols in Fig. 6) collected in the western Gulf later that same day. Where $\Delta^{14}C$=53.3‰ or corresponding to a minimum of 7.5 ppm of added fossil fuel CO_2 from our mixing model, Fig. 7c shows a high emission sensitivity from both MC and an oil and gas producing field in northern Veracruz coupled with a widespread biomass burning influence.

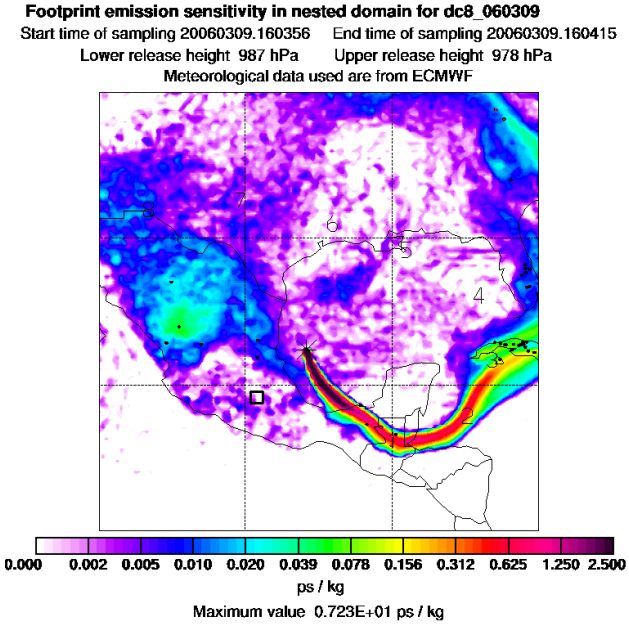

Fig. 7a. FLEXPART footprint emission sensitivity product, averaged over the lowest 100 m, indicating where emissions were likely taken up. Fire hot spots from the MODIS sensor are marked as black dots; red dots if on forested land. Corresponding radiocarbon values are **(a)** 69‰, **(b)** 59‰, and **(c)** 53‰, respectively.

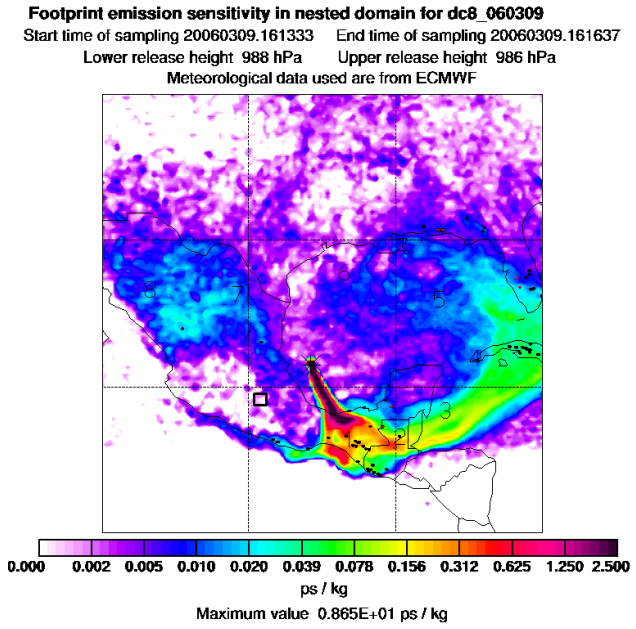

Fig. 7b. Continued.

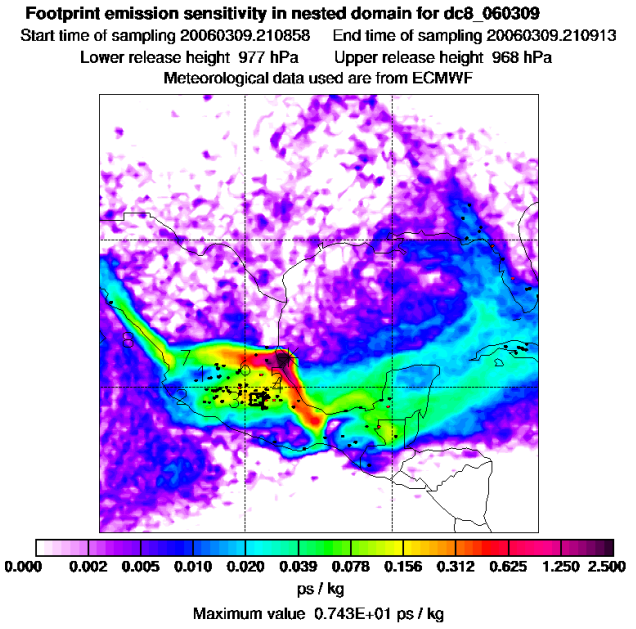

Fig. 7c. Continued.

HCN (582 pptv), ACN (182 pptv), C_2Cl_4 (7 pptv), and C_2H_6 (5371 pptv) mixing ratios are higher than the other 9th March samples, reflecting the proximity to and different relative contributions from the varied emission sources of the two regions. Though these two samples (square symbols Fig. 6) exhibit similar CH_4 mixing ratios, respective CO and CO_2 relationships differ, reflecting interception of an air mass that passed over the petroleum center in SE Mexico then Veracruz (not shown).

The gas released when crude oil is brought to the surface is known as associated gas. Drilling companies routinely flare or vent this material for safety reasons or where no infrastructure exists to bring it to market. Flaring is where the gas is burned and emitted as CO_2, and venting, where the gas is simply released to the atmosphere as CH_4 (Christen, 2004). After CH_4, ethane is the second most abundant constituent of natural gas and both chemical tracers have some common sources: fossil fuel production, biofuel combustion, and biomass burning (Xiao et al., 2008). We examined the CH_4:C_2H_6 molar ratios for these atmospheric observations conducted downwind of these major source regions for source attribution and found CH_4:C_2H_6 ratios (34–114) typical of those for "dry" natural gas fields (i.e. absence of condensate or liquid hydrocarbons) (Xiao et al., 2008). These findings point to the sampling of a complex mixture of emissions attributable to both the venting and flaring of associated gas, fugitive emissions associated with the oil and gas industry, biomass burning, and fossil fuel combustion (based on the isopentane signal) as influences on the radiocarbon content of the atmospheric $\Delta^{14}C$ observations.

3.3 "Hot sources"

Anomalously enriched $\Delta^{14}C$ values (>112‰) were measured in three of the whole air samples, nearly double the radiocarbon in the background atmosphere. The excess levels of ^{14}C cannot be attributed to the release of old bomb carbon from biomass burning as a plausible result using our two-point mixing curve for determination of the relative age of carbon was not realized. The associated CO, CH_4, and CO_2 mixing ratios also do not support a stratospheric influence. The 120‰ value was measured in a sample collected south of MC (Fig. 2) at 2.6 km (i.e. near the altitude of MC or 0.75 km radar altitude) in an atmospheric layer rich in combustion and urban related trace gases The other two highly enriched samples (113‰ and 132‰) were augmented with the biomass burning tracers ACN and HCN yet devoid of an elevated industrial and vehicular emission signature (i.e. C_2Cl_4 or i-pentane), likely a result of sampling on a Sunday (19 March) within a long weekend. These observations were made during a low pass over Monterrey in Nuevo León, and while on approach to MC over the state of Hidalgo, respectively (Fig. 2).

The possible causes of these perturbations in $\Delta^{14}C$ were investigated and a number of potential sources of the emitted radiocarbon identified: production of $^{14}CO_2$ from the boiling water reactors (BWRs) of the Laguna Verde nuclear power plant located in Veracruz; and/or medical and hazardous waste incineration. Mexico has two hazardous waste landfills, 13 fuel blending plants, 11 private hazardous waste incinerators, and 22 medical waste incinerators (Reed et al., 2000). Most of the medical waste incinerators are located in

the Mexico City metropolitan area, although one has been permitted in Monterrey, Nuevo León (Reed et al., 2000). Moreover, Mexico's cement industry has embraced the incineration of hazardous wastes in their cement kilns as an energy recycling strategy. This incineration has been led by the two largest cement producers in Mexico, which have joint ventures with US transnational companies to blend hazardous waste into fuels before burning the waste in their kilns (Reed and Gonzalez, 1997). Twenty one of 30 cement plants throughout Mexico have received either test-burn permits or annual authorizations to burn a variety of hazardous wastes with twelve of these plants located in central Mexico (Reed and Gonzalez, 1997). The locations of some of these potential "hot" point sources are shown in Fig. 2.

The nuclear-waste problem involves not just what existing nuclear power plants produce, but also the low-level radioactive material found in hospitals, universities and in other industries. Most of the ^{14}C released into the environment by incinerators and BWRs is in the form of gaseous emissions (Magnusson et al., 2004) mainly via the stack gas, with CO_2 as the main carrier of ^{14}C. This radiocarbon or "hot source" released into the atmosphere is then available to enter plant carbon pools through photosynthesis or leads to an increase in the local ^{14}C concentration. Previous studies have reported high radiocarbon concentrations (97–184 pMC) in vegetation in areas more than 100 km distant from a nuclear power plant (Mikhajlov et al., 2004) and $\Delta^{14}CO_2$ values 190–6000‰ over background in oak leaves sampled near two hazardous waste incinerators (Trumbore et al., 2002).

We examined 5-day kinematic backward trajectories and several FLEXPART data products calculated along the DC-8 flight tracks for each sampling location and time (not shown) which reveal local influences from the northern and southern sectors of the MCMA for the highest $\Delta^{14}C$ observations, 132‰ and 120‰, respectively. The substantial $^{14}CO_2$ enrichment (113‰) observed near Monterrey also appears to have a local influence south-southwest of the city. From Fig. 2, a close correspondence between these elevated radiocarbon values and local cement kilns is indicated. The transport history of the radiocarbon enriched air parcels consistently reflects an air mass fraction >40% in the ABL 24 h prior to sampling. The numerous and varied potential "hot" point sources located throughout the region complicate source attribution. The observational influence could be attributable to sampling a direct smokestack emission; or from the re-suspension of ^{14}C in contaminated biomass by the pervasive biomass burning occurring during March 2006. The possibility of either scenario exists in our MILAGRO data set and offers a plausible explanation for the anomalously high $\Delta^{14}C$ values observed.

4 Conclusions

Only 23% of the radiocarbon measurements from MILAGRO indicate a distinct fossil fuel influence, an unexpected result for the MCMA sampling environment. Inspection of correlate source tracer species and air mass transport histories suggests that the fossil fuel detection capability of the radiocarbon method was obfuscated by contributions from other local and regional CO_2 sources emitting higher $\Delta^{14}C$ than the background atmosphere. By 2025, the number of megacities is predicted to reach twenty seven, with the majority located in the developing world, each with their own unique emission signatures, all likely major sources of atmospheric CO_2. Observations during MILAGRO have shown the complexity of radiocarbon cycling in the megacity environment within a developing country and indicate adding detailed simultaneous measurements of other chemical tracers to the isotopic marker ^{14}C are highly desirable for better evaluation of the various sources contributing to the total measured CO_2 signal.

Acknowledgements. We thank Charlie Hudgins, Jim Plant, and the NASA DC-8 flight crew for their valuable contributions during INTEX-B. We are grateful to NOAA ESRL for the MLO and NWR data, and Andreas Stohl for the FLEXPART data products. We also gratefully acknowledge funding support from the NASA Tropospheric Chemistry Program and the W. M. Keck Foundation for a major research instrumentation grant.

Edited by: J. Gaffney

References

Amiro, B. D., Todd, J. B., Wotton, B. M., Logan, K. A., Flannigan, M. D., Stocks, B. J., Mason, J. A., Martell, D. L., and Hirsch, K. G.: Direct carbon emissions from Canadian forest fires, 1959–1999, Can. J. Forest Res., 31, 512–525, 2001.

Anderson, B. E., Gregory, G. L., Collins Jr., J. E., Sachse, G. W., Conway, T. J., and Whiting, G. P.: Airborne observations of spatial and temporal variability of tropospheric carbon dioxide, J. Geophys. Res., 101, 1985–1997, 1996.

Blake, D. R and Rowland, F. S.: Urban leakage of Liquefied Petroleum Gas and its Impact on Mexico City Air Quality, Science, 269, 953–956, 1995.

Blake, D. R., Chen, T.-Y., Smith, T. W. Jr., Wang, C. J.-L., Wingenter, O. W., Blake, N. J., and Rowland, F. S.: Three-dimensional distribution of nonmethane hydrocarbons and halocarbons over the northwestern Pacific during the 1991 Pacific Exploratory Mission (PEM-West A), J. Geophys. Res., 101(D1), 1763–1778, 1996.

Caldeira, K., Rau, G. H., and Duffy, P. B.: Predicted net efflux of radiocarbon from the ocean and increase in atmospheric radiocarbon content, Geophys. Res. Lett., 25, 3811–3814, 1998.

Christen, K.: Environmental Impacts of Gas Flaring, Venting add up, Environ. Sci. Technol., p. 480A, doi:10.1021/es0406886, 15 December 2004.

Collins, C. O. and Scott, S. L.: Air Pollution in the Valley of Mexico, Geogr. Rev., 83(2), 119–133, 1993.

Crounse, J. D., DeCarlo, P. F., Blake, D. R., Emmons, L. K., Campos, T. L., Apel, E. C., Clarke, A. D., Weinheimer, A. J., McCabe, D. C., Yokelson, R. J., Jimenez, J. L., and Wennberg, P. O.: Biomass burning and urban air pollution over the Central Mexican Plateau, Atmos. Chem. Phys. Discuss., 9, 2699–2734, 2009, http://www.atmos-chem-phys-discuss.net/9/2699/2009/.

De Bauer, L. I. and Krupa, S. V.: Valley of Mexico: summary of observational studies on its air quality and effects on vegetation, Environ. Pollut., 65, 109–118, 1990.

Dutta, K.: Coherence of tropospheric $^{14}CO_2$ with El Nino/Southern Oscillation, Geophys. Res. Lett., 29(20), 1987, doi:10.1029/2002GL014753, 2002.

Gaffney, J. S., Marley, N. A., Tackett, M., Gunawan, G., Sturchio, N. C., Heraty, L., Martinez, N., Hardy, K., and Guilderson, T.: Biogenic Carbon Dominance Based on 13C/12C and 14C Measurements of Total Carbon at T-0 and T-1 Sites during MILAGRO, 88th National Meeting of the American Meteorological Society, Tenth Conference on Atmospheric Chemistry, Conference Proceedings Volume, Paper J1.1, 5 pp. online available at: http://ams.confex.com/ams/pdfpapers/131852.pdf, 2008.

Hsueh, D. Y., Krakauer, N. Y., Randerson, J. T., Xu, X., Trumbore, S. E., and Southon, J. R.: Regional patterns of radiocarbon and fossil fuel-derived CO_2 in surface air across North America, Geophys. Res. Lett., 34, L02816, doi:10.1029/2006GL027032, 2007.

Kitagawa, H., Mukai, H., Nojiri, Y., Shibata, Y., Kobayashi, T., and Nojiri, T.: Seasonal and secular variations of atmospheric $^{14}CO_2$ over the western pacific since 1994, Radiocarbon, 46, 901–910, 2004.

Levin, I., Munnich, K. O., and Weiss, W.: The effect of anthropogenic CO_2 and ^{14}C sources on the distribution of ^{14}C in the atmosphere, Radiocarbon, 22(2), 379–391, 1980.

Levin, I. and Hesshaimer, V.: Radiocarbon – A unique tracer of global carbon cycle dynamics, Radiocarbon, 42, 69–80, 2000.

Levin, I. and Kromer, B.: The tropospheric $^{14}CO_2$ level in mid-latitudes of the northern hemisphere (1959–2003), Radiocarbon, 46, 1261–1272, 2004.

Magnusson, Å., Stenström, K., Skog, G., Adliene, D., Adlys, G., Hellborg, R., Olariu, A., Zakaria, M., Rääf, C., and Mattsson, S.: Levels of ^{14}C in the terrestrial environment in the vicinity of two European nuclear power plants, Radiocarbon, 46(2), 863–868, 2004.

Marley, N. A., Gaffney, J. S., Tackett, M., Sturchio, N. C., Heraty, L., Martinez, N., Hardy, K. D., Marchany-Rivera, A., Guilderson, T., MacMillan, A., and Steelman, K.: The impact of biogenic carbon sources on aerosol absorption in Mexico City, Atmos. Chem. Phys., 9, 1537–1549, 2009, http://www.atmos-chem-phys.net/9/1537/2009/.

Mikhajlov, N., Kolkovskij, V., Pavlova, I., and Luchina, G.: Radiocarbon in elements of the Landscape (Belarus), Geochronometria, 23, 59–66, 2004.

Molina, L. T., Madronich, S., Gaffney, J. S., and Singh, H. B.: Overview of MILAGRO/INTEX-B Campaign, IGAC News Letter, 38, 2–15, April 2008.

Mook, W. G.: The effect of fossil fuel and biogenic CO_2 on the ^{13}C and ^{14}C content of atmospheric carbon dioxide, Radiocarbon, 22, 392–397, 1980.

Pataki, D. E., Alig, R. J., Fung, A. S., Golubiewski, N. E., Kennedy, C. A., McPherson, E. G., Nowak, D. J., Pouyat, R. V., and Lankao, P. R.: Urban ecosystems and the North American carbon cycle, Glob. Change Biol., 12, 2092–2102, doi:10.1111/j.1365-2486.2006.01242.x, 2006.

Raga, G. B., Baumagardner, D., Castro, T., Martinez-Arroyo, A., and Navarro-Gonzalez, R.: Mexico City air quality: a qualitative review of gas and aerosol measurements (1960–2000), Atmos. Environ., 35, 4041–4058, 2001.

Randerson, J. T., Enting, I. G., Schuur, E. A. G., Caldeira, K., and Fung, I. Y.: Seasonal and latitudinal variability of troposphere $\Delta^{14}CO_2$: Post bomb contributions from fossil fuels, oceans, the stratosphere, and the terrestrial biosphere, Global Biogeochem. Cy., 16(4), 1112, doi:10.1029/2002GB001876, 2002.

Reed, C. and Gonzalez, F. B.: Exporting Dirty Technologies: Mexican Cement Kilns Begin Burning Hazardous Wastes, Border-Lines, 36, 5(6), online available at: http://americas.irc-online.org/borderlines/1997/bl36/bl36dirt.html, June 1997.

Reed, C., Jacott, M., and Villamar, A.: Hazardous Waste Management in the United States-Mexico Border States: More Questions than Answers, Texas Center for Policy Studies, Austin Texas, online available at: http://www.texascenter.org/publications/haz2000.pdf, 2000.

Rozanski, K., Levin, I., Stock, J., Falcon, R. E. G., and Rubio, F.: Atmospheric $^{14}CO_2$ variations in the equatorial region, 15th International ^{14}C Conference, Radiocarbon, 37, 509–515, 1995.

Sachse, G. W., Harriss, R. C., Fishman, J., Hill, G. F., and Cahoon, D. R.: Carbon monoxide over the Amazon basin during the 1985 dry season, J. Geophys. Res., 93, 1422–1430, 1988.

Singh, H. B., Salas, L., Herlth, D., Kolyer, R., Czech, E., Viezee, W., Li, Q., Jacob, D. J., Blake, D., Sachse, G., Harward, C. N., Fuelberg, H., Kiley, C. M., Zhao, Y., and Kondo, Y.: In situ measurements of HCN and CH_3CN over the Pacific Ocean: Sources, sinks, and budgets, J. Geophys. Res., 108(D20), 8795, doi:10.1029/2002JD003006, 2003.

Singh, H. B., Brune, W. H., Crawford, J. H., Flocke, F., and Jacob, D. J.: Chemistry and transport of pollution over the Gulf of Mexico and the Pacific: spring 2006 INTEX-B campaign overview and first results, Atmos. Chem. Phys., 9, 2301–2318, 2009, http://www.atmos-chem-phys.net/9/2301/2009/.

Southon, J., Santos, G., Druffel-Rodriguez, K., Druffel, E., Trumbore, S. E., Xu, X. M., Griffin, S., Ali, S., and Mazon, M.: The Keck Carbon Cycle AMS Laboratory, University of California, Irvine: Initial operation and a background surprise, Radiocarbon, 46, 41–49, 2003.

Stohl, A., Hittenberger, M., and Wotawa, G.: Validation of the Lagrangian particle dispersion model FLEXPART against large scale tracer experiments. Atmos. Environ., 32, 4245–4264, 1998.

Stohl, A., Eckhardt, S., Forster, C., James, P., Spichtinger, N., and Seibert, P.: A replacement for simple back trajectory calculations in the interpretation of atmospheric trace substance measurements, Atmos. Environ., 36, 4635–4648, 2002.

Stone, E. A., Snyder, D. C., Sheesley, R. J., Sullivan, A. P., Weber, R. J., and Schauer, J. J.: Source apportionment of fine organic aerosol in Mexico City during the MILAGRO experiment 2006, Atmos. Chem. Phys., 8, 1249–1259, 2008, http://www.atmos-chem-phys.net/8/1249/2008/.

Stuiver, M. and Polach, H. A.: Reporting of ^{14}C data, Radiocarbon, 19, 355–363, 1977.

Stuiver, M. and Quay, P. D.: Atmospheric ^{14}C changes resulting

from fossil fuel CO_2 released and cosmic ray flux variability, Earth Planet. Sci. Lett., 53, 349–362, 1981.

Suess, H. E.: Radiocarbon concentration in modern wood, Science, 122, 415–417, 1955.

Tans, P. P., deJong, A. F. M., and Mook, W. G.: Natural atmospheric ^{14}C variation and the Suess effect, Nature, 280, 826–828, 1979.

Trumbore, S., Gaudinski, J. B., Hanson, P. J., and Southon, J. R.: Quantifying Ecosystem Atmosphere Carbon Exchange with a ^{14}C label, EOS, Trans. AGU, 83(24), 11 June 2002.

Turnbull, J. C., Miller, J. B., Lehman, S. J., Tans, P. P., Sparks, R. J., and Southon, J.: Comparison of $^{14}CO_2$, CO, and SF_6 as tracers for recently added fossil fuel CO_2 in the atmosphere and implications for biological CO_2 exchange, Geophys. Res. Lett., 33, L01817, doi:10.1029/2005GL024213, 2006.

Turnbull, J. C., Lehman, S. J., Miller, J. B., Sparks, R. J., Southon, J. R., and Tans, P. P.: A new high precision $^{14}CO_2$ time series for North American continental air, J. Geophys. Res., 112, D11310, doi:10.1029/2006JD008184, 2007.

Turnbull, J. C., Miller, J. B., Lehman, S. J., Hurst, D., Peters, W., Tans, P. P., Southon, J., Montzka, S. A., Elkins, J. W., Mondeel, D. J., Romashkin, P. A., Elansky, N., and Skorokhod, A.: Spatial distribution of $\Delta^{14}CO_2$ across Eurasia: measurements from the TROICA-8 expedition, Atmos. Chem. Phys., 9, 175–187, 2009, http://www.atmos-chem-phys.net/9/175/2009/.

Tyler, S. C., Ajie, H. O., Gupta, M. L., Cicerone, R. J., Blake, D. R., and Dlugokencky, E. J.: Carbon isotopic composition of atmospheric methane: A comparison of surface level and upper tropospheric air, J. Geophys. Res., 104, 13895–13910, 1999.

Vay, S. A., Anderson, B. E., Conway, T. J., Sachse, G. W., Collins Jr., J. E., Blake, D. R., and Westberg, D. J.: Airborne observations of the tropospheric CO_2 distribution and its controlling factors over the South Pacific Basin, J.Geophys. Res., 104(D5), 5663–5676, 1999.

Vay, S. A., Woo, J.-H., Anderson, B. E., Thornhill, K. L., Blake, D. R., Westberg, D. J., Kiley, C. M., Avery, M. A., Sachse, G. W., Streets, D. G., Tsutsumi, Y., and Nolf, S. R.: Influence of regional-scale anthropogenic emissions on CO_2 distributions over the western North Pacific, J. Geophys. Res., 108(D20), 8801, doi:8810.1029/2002JD003094, 2003.

Wiedinmyer, C. and Neff, J. C.: Estimates of CO_2 from fires in the United States: implications for carbon management, Carbon Balance Management, 2(10), doi:10.1186/1750-0680-1182-1110, online available at: http://www.cbmjournal.com/content/2/1/10, 2007.

Xiao, Y., Logan, J. A., Jacob, D. J., Hudman, R. C., Yantosca, R., and Blake, D. R.: Global budget of ethane and regional constraints on U.S. sources, J. Geophys. Res., 113, D21306, doi:10.1029/2007JD009415, 2008.

Xu, X., Trumbore, S., Ajie, H., Tyler, S., Randerson, J., and Krakauer, N.: Atmospheric $^{14}CO_2$ over the mid Pacific Ocean and at Point Barrow, Alaska, USA from 2002 to 2004, EOS Trans. AGU, 85(47), Fall Meet. Suppl., Abstract B23A-0948, 2004.

Xu, X., Trumbore, S. E., Ajie, H. O., and Tyler, S. C.: $\Delta^{14}C$ of atmospheric CO_2 over the subtropical and equatorial Pacific from Fall 2002 to Winter 2004, 19th International Radiocarbon Conference, Oxford, UK, 2006.

Yokelson, R. J., Goode, J. G., Ward, D. E., Susott, R. A., Babbitt, R. E., Wade, D. D., Bertschi, I., Griffith, D. W. T., and Hao, W. M.: Emissions of formaldehyde, acetic acid, methanol, and other trace gases from biomass fires in North Carolina measured by airborne Fourier transform infrared spectroscopy, J. Geophys. Res., 104(D23), 30109–30125, 1999.

Yokelson, R. J., Urbanski, S. P., Atlas, E. L., Toohey, D. W., Alvarado, E. C., Crounse, J. D., Wennberg, P. O., Fisher, M. E., Wold, C. E., Campos, T. L., Adachi, K., Buseck, P. R., and Hao, W. M.: Emissions from forest fires near Mexico City, Atmos. Chem. Phys., 7, 5569–5584, 2007, http://www.atmos-chem-phys.net/7/5569/2007/.

Zondervan, A. and Meijer, H. A. J.: Isotopic characterisation of CO_2 sources during regional pollution events using isotopic and radiocarbon analysis, Tellus, 48B, 601–612, 1996.